Critical Current in Various Pinning Landscapes

Andreas Glatz[1], Igor Aronson[1], George Crabtree[1], Alexei Koshelev[1], Ivan Sadovsky[1], Dmitry Karpeev[2], Carolyn Phillips[2]
[1]Materials Science Science Division, Argonne National Laboratory, Argonne, IL 60439, USA
[2]Mathematics and Computer Division, Argonne National Laboratory, Argonne, IL 60439, USA

oscon-scidac.org

GL model & Motivation

Time-dependent Ginzburg-Landau

TDGL equations:

$$\frac{\partial\Psi}{\partial t} = -\frac{\delta\mathcal{F}_{\rm GL}}{\delta\Psi^*}\,,\quad \frac{\delta\mathcal{F}_{\rm GL}}{\delta\mathbf{A}} = 0$$

In dimensionless units:

$$u(\partial_t + i\mu)\psi = \epsilon(\mathbf{r})\psi - |\psi|^2\psi + (\nabla - i\mathbf{A})^2\psi + \zeta(\mathbf{r},t)$$
$$\kappa^2\nabla\times(\nabla\times\mathbf{A}) = \mathbf{J}_n + \mathbf{J}_s + \mathcal{I},$$

Coupled system for ψ and $\mathbf{A}$:
- ψ — complex order parameter characterizing density of Cooper pairs
- $\mathbf{A}$ — vector potential for magnetic field
- ζ and $\mathcal{I}$ — thermal fluctuations
- $\epsilon(\mathbf{r}) = \frac{T_c(\mathbf{r})-T}{T} \to 0$ for $T \to T_c$ (critical temperature)

Total current: $J=J_s+J_n$ $\quad \mathbf{J} = \mathrm{Im}\left[\psi^*(\nabla - i\mathbf{A})\psi\right] - (\nabla\mu + \partial_t\mathbf{A})$

OSCon: Robust optimization of pinning & geometry for high critical currents and resulting energy applications
- *Critical current determined by long-time evolution of TDGL (to stationary flow)*
- *Dominated by rare events of vortex depinning, avalanches, nucleation and splitting & reconnection*
- *Frequency and duration of pinning/depinning depends on configurations of inclusions*
- *Suitable pinning configurations must be determined using geometry optimization*

Modeling of pinning

Here: Regular simulation grid (on GPUs)

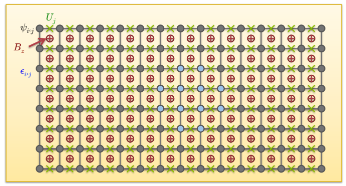

T_c modulation: Inclusions and pinning

Inclusions and defects are modeled by T_c modulation → corresponding to normal metallic pinning centers: spatial variation of $\epsilon(\mathbf{r})$ [positive in the superconductor, negative in the defect]
- arbitrary geometry
- on a regular grid

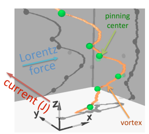

Example: regular 2D hole array with modulation of the linear coefficient $\epsilon(\mathbf{r})$, where $T>T_c$ in the "holes"

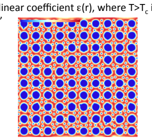

Random spherical inclusions

2nd type of inclusions: insulators → modeled by zero-normal-supercurrent boundary conditions
- Most appropriate on unstructured meshes (see poster 2)
- On regular meshes normal to mesh edges (in progress)

Critical currents for spherical (metallic) inclusions

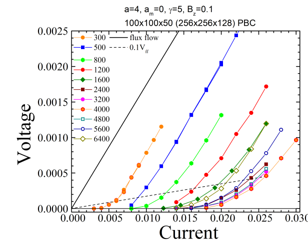

Current-voltage characteristics for different inclusion concentrations (inclusions are randomly distributed in the simulation volume: the critical current is determined by a fraction of the corresponding free flux flow voltage

Instead of the concentration, the volume fraction and inclusion diameter are the two parameters characterizing the random spherical pinning landscape.

Critical current also depends on magnetic field:

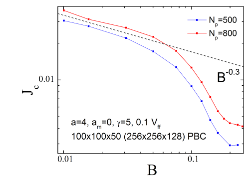

Optimal critical current

B = 0.05 B_{c2}

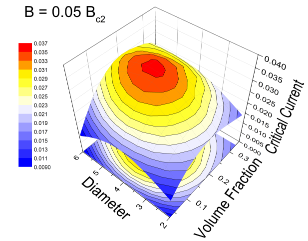

Parallel fields

Experimental result: MoGe slap with parallel current and field

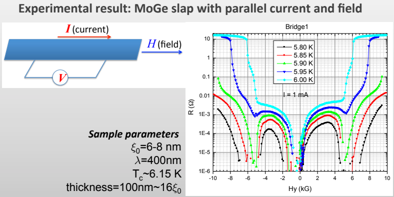

Numerical realization

- Sample is discretized using a regular mesh of 512x128x32 grid points with mesh size of $\xi_0/2$ → realistic thickness
- Sample is periodic in x-direction
- Inclusions are modeled by a different low-T_c component
- 0-100 spherical inclusions with diameter $5\xi_0$ are randomly placed in the volume → average over different disorder realizations
- A fixed constant current is applied in x-direction as well as a variable magnetic field
- *Simulation time:* 25mill time steps for 100 field values

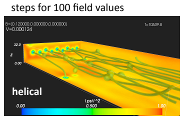

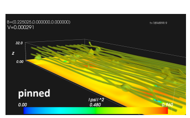

Helical motion & Reentrance

Magnetic field & voltage for one disorder configuration

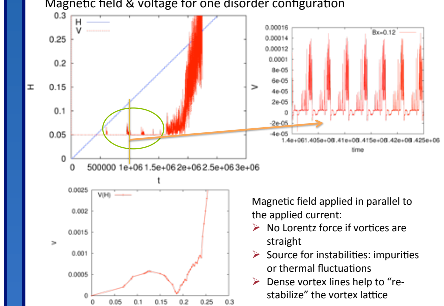

Magnetic field applied in parallel to the applied current:
- No Lorentz force if vortices are straight
- Source for instabilities: impurities or thermal fluctuations
- Dense vortex lines help to "re-stabilize" the vortex lattice

New discovery: a new periodically "rotating" vortex state appears at intermediate field strength having finite resistance

Visualization using location of inclusions and vortex detection results (see poster 3)

Competing defects

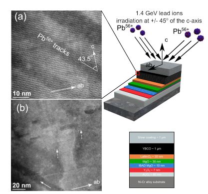

Commercial superconducting tape with nanorod inclusions is irradiated by heavy ions at 45 deg → understanding of the critical current depending on the angle of the external magnetic field

Simulation

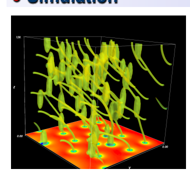

Vortex configuration with nanorods

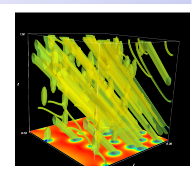

Nanorods & Irradiated columnar defects

Two new extensions to the main simulations code required:
- Arbitrary external magnetic field direction
- Rotation-symmetric (cylindrical) integration domain

Results

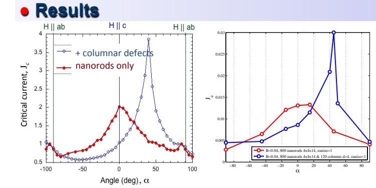

Left: Experimental $J_c(\alpha)$ dependence. *Right:* Numerical $J_c(\alpha)$ dependence. Red (nanorods) and blue (nanorods + columnar defects) lines are calculated slightly below the matching field of the system.

- **The effects from different defects are not additive.** Additional defects can simultaneously decrease the critical current at some directions of the magnetic field and increase it at other directions.
- **The alignment of the dominant inclusions define peaks.** In case of nanorods the peak of $J_c(\alpha)$ is observed at α = 0° and in the case of dominating continuous columnar defects it is α = 45°.
- **The peak at α = 0° decreases.** The critical current in systems with nanorods is larger then the one in the system with nanorods and columnar defects at α = 0°. In the former case it is obvious that the pinning is best as the defects a longest parallel to the vortices. On the other hand, continuous cylindrical inclusions allow vortices to move creating "rails" across the system.

→ *Close to quantitative agreement of experimental results and explanation of the underlying mesoscopic mechanisms*